Nonlocal Interactions Stabilize Long Range Loops in the Initial Folding Intermediates of Reduced Bovine Pancreatic Trypsin Inhibitor†

Varda Ittah and Elisha Haas*

Department of Life Sciences, Bar-Ilan University, Ramat Gan 52900, Israel

Received August 18, 1994; Revised Manuscript Received December 12, 1994®

ABSTRACT: A search for the topology of the chain folding of reduced bovine pancreatic trypsin inhibitor (BPTI), in unfolded and partially folded states, was done by means of time resolved dynamic nonradiative excitation energy transfer (ET) measurements. Four double labeled BPTI derivatives were used in which the donor was attached to the N-terminal arginine residue and the acceptor was specifically attached to one of the lysine residues. The four derivatives form a series of labeled backbone segments of increasing length spanning the full lengths of the BPTI chain: 15, 26, 41, and 46 residues. The intramolecular segmental end-to-end distance (EED) distributions were determined for all the derivatives by global analysis of the decay curves of both the donor and the acceptor in the reduced state, in low (0.5 M) guanidinium chloride (GuHCl) concentrations at pH 3.6 and 2.1 (R and A states, respectively). The results show that, in the partial folding conditions of low GuHCl concentration, reduced BPTI is in a compact state, but in this state the polypeptide chain is not in a condensed statistical coil conformation. Two distinct subpopulations were found for the four intramolecular EED distributions. One subpopulation was compact, with native-like EED distribution, while the second was unfolded. The pairs of sites, residues 1 and 26 and residues 1 and 46, showed close proximity in the dominant subpopulation. These contacts form two loops (probably collapsed): one consists of the first 26 residues, and the second comprises the full length of the chain from the N- to the C-terminal segments, which is in fact made up to two shorter loops (1−26 and 27−46). The N-terminal 15 residue segment was relaxed into statistical coil-like non-native conformation, in contrast to its extended conformation in the native state. The effect of temperature in the range of 2−60 °C was small; the folded subpopulations were stable over this range. These results show that in BPTI the compact conformations found under unfolding and partially folding conditions have native-like chain topology. Under the conditions of transition to partially folding conditions the compact conformation is stabilized, not only by the hydrophobic collapse and the local interaction but also by nonlocal interactions (NLIs). Few specific, very stable NLIs between the three segments which form the main structural elements of the native conformation direct the formation of native-like topology of the chain in the transition. These interactions form loops of the chain segments whose ends are held in close proximity by the strong NLIs. The stabilization of closed loops of chain segments can be a very effective early step in the folding of BPTI. These observations are interpreted as an indication that, in unfolded BPTI, stabilization of long range loops by specific NLIs can facilitate the accelerated folding into a native topology, within the early steps of the folding pathway. Formation of loops is a very effective mean of reducing chain entropy at the expense of a minimal number of very stable interactions.

The well-known Levinthal paradox (Levinthal, 1968) led to the conclusion that proteins fold via pathways of folding. This proposal stimulated the intense search for intermediate structures formed along the pathway. Much attention has been directed to the formation of secondary structures, the compact molten globule (MG)[1] and disulfide-pairing intermediate structures (Creighton, 1978; Harrison & Durbin, 1985; Karplus & Weaver, 1976; Kim & Baldwin, 1990; Matthews, 1991; Montelione & Scheraga, 1989; Sancho et al., 1992; Schmid, 1992; Shortle, 1993; Weissman & Kim, 1992). The molten globule (MG) state has been shown to exist under partially folding conditions in many proteins (Kuwajima, 1989; Ptitsyn, 1987; Uversky et al., 1992). General electrostatic effects in proteins (Goto & Fink, 1989; Goto et al., 1990; Stiger et al., 1991; Yang & Honig, 1992), and the effect of pH and salt concentrations were shown to influence the MG state (Goto & Fink, 1990). Upon lowering the pH and/or increasing the ionic strength, the MG state, defined as the A state, can be achieved in several proteins. A theory explaining this phenomenon (Alonso et al., 1991)

† This work was supported by the NIH National Institute of General Medical Sciences Grant GM 39372, by the US-ISRAEL Binational Science Foundation (Grant 91-170), and by equipment grants from the Basic Research Fund of the Israeli Academy of Sciences (1984, 1988, 1990) and from the Russle Foundation of Miami Beach, FL. V.I. holds an Eshkol fellowship.

® Abstract published in *Advance ACS Abstracts,* March 1, 1995.

[1] Abbreviations: (1−*n*)BPTI, N^{α}MNA-Arg^{1}-N^{ϵ}-(DA-coum)-Lys^{n}-BPTI; (DA-coum)$_2$-BPTI, BPTI labeled by two DA-coum groups; (MNA)$_2$-BPTI, BPTI labeled by two MNA groups; BPTI, bovine pancreatic trypsin inhibitor; DA-coum-BPTI, BPTI labeled by single DA-coum groups; DA-coum [7-(dimethylamino)coumarin-4-yl]acetyl; DTT, dithiothriethol; *E*, transfer efficiency (%); EED, end-to-end distance; ET, energy transfer; FWHM, full width at half-maximum; GuHCl, guanidinium chloride; LI, local interaction; MA/MCP, multianode microchannel plate; MG molten globule; MNA, (2-methoxynaphthyl)methylenyl; NLI, nonlocal interaction; PMT, photomultiplier tube; R(1−*n*)BPTI, reduced (1−*n*)BPTI; R-BPTI, reduced BPTI; SNR, signal to noise ratio.

0006-2960/95/0434-4493$09.00/0

predicts a more prominent compact state for shorter proteins.

The concept of the folding pathway leads to the hypothesis that the initial conformational transitions are of key importance in determination of the direction of the pathway. The common experimental approach to the problem of elucidation of the pathway of folding is based on unfolding of a protein by a perturbation and monitoring the sequence of conformational changes initiated by elimination of the perturbation. Several mixing experiments show that the rates of the initial conformational transitions are shorter than the dead time of the stopped flow devices (Chaffotte et al., 1992). Thus, determination of the structure of such transient mixtures of partially folded populations of molecules is not practical, and much attention is given to investigation of the conformation of protein samples under conditions of various levels of conformational perturbation, e.g., denaturant concentrations. The underlying assumption is that the structures stabilized by the initial relief of the perturbation are related to the structures which are stabilized initially in time dependent experiments, in which the protein is jumped into folding conditions (Shortle, 1993; Uversky et al., 1992). The first question to be asked is whether under the conditions considered "unfolding" (e.g., high concentration of denaturants) the protein is indeed unfolded. Several experiments were reported which showed that denatured proteins are not necessarily unfolded (Amir & Haas, 1987; Amir et al., 1992; Dill & Shortle, 1991; Dobson, 1991; Gottfried & Haas, 1992; James et al., 1992; Neri et al., 1992; Roeder et al., 1988; Shortle et al., 1989; Tanford, 1968; Sosnik & Trewhella, 1992). In most experiments it has been shown that chemically denatured proteins have a compact average conformation with "residual structure". Elucidation of the residual structures is of great interest since they can function as chain folding initiation structures (CFIS) (Montelione & Scheraga, 1989). So far most experiments detected the existence of local residual structures. But the main question raised by the Leventhal paradox is the path to the generation of the native-like overall topology of the backbone chain of the protein. This requires long range distance determinations which can be used to characterize the topology of subdomain and the overall conformation by combination of a series of distances. Therefore, nonradiative excitation energy transfer (ET) (Förster, 1948; Stryer & Haugland, 1967; Haas et al., 1975) between probes attached to well-defined sites on a polypeptide chain was introduced as a sensitive method for detection of intramolecular segmental end-to-end distance (EED) distributions in folding intermediates of globular proteins (Amir & Haas, 1987; Gottfried & Haas, 1992; Haas, 1986).

BPTI, which contains 3 disulfide bonds and 58 amino acid residues, has been widely used as a model protein for folding research by many methods including X-ray crystallography (Deisenhofer & Steigemann, 1975; Wlodawer et al., 1984; Wlodawer et al., 1987), NMR (Masson & Wüthrich, 1973; Karplus et al., 1973; Berndt et al., 1992), two-dimensional NMR (Wagner et al., 1987), hydrogen exchange (Tüchsen & Woodward, 1987), and theoretical calculations (Levitt, 1983; Daggett & Levitt, 1992; Manning & Woody, 1989). Formation of native BPTI from its reduced state, by forming disulfide bridges, has been investigated (Creighton, 1978, 1980, 1984, 1986; Weissman & Kim, 1991, 1992). Theoretical aspects of disulfide bond formation were also examined (Kobayashi et al., 1992). More recently, site directed mutagenesis combined with various other methods has been used in studies of the folding pathway of BPTI (Danishefsky et al., 1993; Darby et al., 1991, 1992; Goldenberg & Zhang, 1993; Goldenberg et al., 1992; Hausset et al., 1991; Hurle et al., 1990; Van Mierlo et al., 1993).

The emerging picture is that even when a single disulfide bond is formed, the backbone of BPTI is essentially already folded into a native-like topology. Therefore attempts to elucidate the truly initial steps of folding should be directed at the reduced states of BPTI. ORD measurements of reduced BPTI have shown that it lacks any elements of secondary structure or a cooperative thermal transition (Gussakovsky & Haas, 1992). 2-D NMR experiments (Lumb & Kim 1994) using a model of reduced BPTI confirmed this observation and revealed evidence for localized hydrophobic clustering in which only the side chains of residues 19 and 21 are involved. Yet, time resolved dynamic ET measurements of labeled BPTI derivatives reduced in high concentrations of guanidinium chloride (GuHCl) showed that a significant subpopulation of the unfolded molecules have compact conformations with native-like intramolecular distances. This observation leads to the hypothesis that *nonlocal interactions (NLIs) which do not depend on preexisting secondary structure elements can stabilize native-like subdomain folds in unfolded BPTI.* The aim of the present work was to follow the development of the formation of native-like or non-native-like topological details in the structure of reduced BPTI early in the folding pathway. The approach chosen was stepwise reduction of the denaturant concentration or pH combined with time resolved ET measurements under each set of conditions. The short range goal was to analyze the topology of the protein backbone in the early intermediates and in a possible compact molten globule (MG) in order to search, in the long run, for the chain segments or side chains directly responsible for stabilization of native-like subdomain structures in the early folding intermediates.

The work reported here was done by preparing a series of four fluorescently labeled BPTI derivatives, $(1-n)$BPTI, (n = 15, 26, 41, 46), in which a (2-methoxy-1-naphthyl)-methylenyl group (MNA) was attached to the α-amino group of arginine, at position 1, and a [7-(dimethylamino)coumarin-4-yl]acetyl group (DA-coum) was specifically attached via an amide bond, to a single ϵ-amino group of one of the four lysine residues at positions 15, 26, 41, or 46 (Amir & Haas, 1987). This method has been described previously (Haas, 1986; Amir & Haas, 1988; Amir et al., 1992; Gottfried & Haas, 1992).

In the present work the ET method and labeled BPTI derivatives were used to search for the topological characteristics of the compact states of BPTI in several acidic conditions and in the presence of low concentrations of GuHCl. Four intramolecular EED distributions were determined in each state. The results show that there are conformational subpopulations in the compact partially folded states of BPTI and that one of the two is generally native-like, while the other is unfolded. They show that the compact conformation of BPTI in the partially folding conditions under the influence of the hydrophobic collapse is not in a state of a condensed statistical coil. It has a native-like topology which is stabilized by the combination of local interactions and a few nonlocal interactions (NLIs), which form loops in the backbone of the protein and direct the protein into its native-like topology, even in the absence of any disulfide bonds.

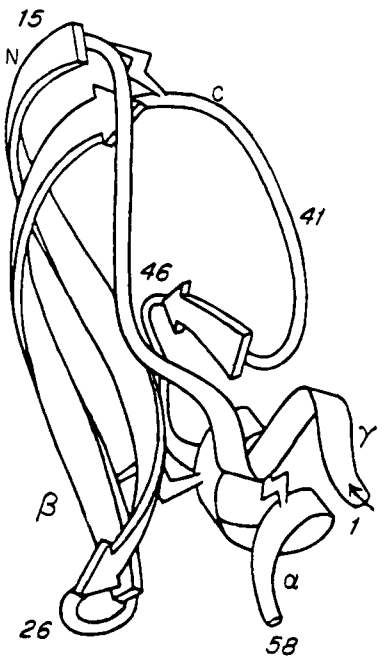

FIGURE 1: The native structure of BPTI. The residues labeled by the probes are marked with the residue numbers. α, β, and γ indicate the three chain segments which in the native state form the structural elements. These are referred to in the next not as secondary structures but as names for the corresponding chain segments only. "N" and "C" mark the two loops formed between γ and β and β and α, respectively.

MATERIALS AND METHODS

Sample Preparation. Singly- and doubly-labeled BPTI derivatives were prepared, purified, and characterized as described previously (Amir & Haas, 1987). Briefly, the method of labeling was based on nonselective reductive alkylation of the amino groups with 2-methoxynaphthalene-1-aldehyde. The mixture of labeled products was first fractionated by affinity chromatography on trypsin−Sepharose (which yielded the derivative labeled at lysine 15). A second purification step based on reversed phase HPLC yielded pure derivative labeled at the α-amino group of the N-terminal arginine. This derivative was again labeled nonselectively by acylation with [7-(dimethylamino)coumarin-4-yl]acetyl *N*-hydroxysuccinimide ester. The mixture of products was separated by a second cycle of affinity chromatography and reversed phase HPLC separations. Four double-labeled BPTI derivatives were obtained in which the donor probe (2-methoxy-1-naphthyl)methylenyl (MNA) was attached to the α-amino group of residue 1, while the acceptor was attached to the ϵ-amino group of one (and only one) of four lysine residues at positions 15, 26, 41, and 46. The structure and purity of the derivatives were analyzed by peptide mapping and UV spectroscopy. All four derivatives were active like the native protein (except for the (1−15)BPTI which had a reduced inhibitory activity). The kinetics of unfolding of the last three derivatives (labeled at residues 26, 41, and 46) were 3 times faster than the native unlabeled protein, with minor differences between them. The thermal stabilities of the four derivatives were very close, with small variations of 0.5 kcal/mol between them. Figure 1 shows a schematic drawing of the protein with the labeling sites.

Protein samples were reduced and denatured overnight in a buffer solution containing 50 mM bicine (Sigma), pH 8, 20 mM dithiothreitol (DTT, Sigma), 1 mM EDTA (Fluka), and 6 M GuHCl. The protein sample was diluted 12-fold with 60 mM format buffer (prepared with formic acid from Merck), pH 3.7, 4 mM DTT, and 1 mM EDTA to achieve a concentration of 0.5 M GuHCl at pH 3.6; or with 50 mM glycine buffer (Sigma) pH 2, 4 mM DTT, and 1 mM EDTA to achieve a concentration of 0.5 M GuHCl at pH 2.1. To remove all the salt from the solution, the reduced denatured sample was passed through a Bio-Gel P-2, 100−200 mesh (wet), 2 cm column (Bio-Rad Laboratories), and the appropriate fraction was collected for measurements. Sample concentrations were 1−2 μM. At these concentrations it was found that the protein did not form aggregates at any of the above conditions. All reagents used in this work were of analytical grade or higher. Measurements were done with freshly prepared solutions. Fluorescence emission spectra were measured using an ISS-GregPC spectrofluorometer. Fluorescence spectra were recorded before and after each time resolved fluorescence measurement in order to make sure that the samples did not change during the experiment.

Experimental Design. The time-correlated single photon counting system used for our measurements was described previously (Gottfried & Haas, 1992). Briefly, it consists of a mode-locked, frequency doubled Nd:YAG laser (coherent Antares 76-YAG) used to synchronously pump a dye laser (Coherent 701-2CD) with rhodamine 6G (Exiton) as a dye. The 2 MHz, 5 ps out-coming pulse was focused onto a BBO type I crystal (CSK Co., Inc.) to generate pulses in the UV range with up to 0.3 mW. The light was passed through a double Fresnel rhomb (Optics for Research) to rotate it to the desired angle and then excite the sample in a custom-made cylindrical quartz cell of 5-mm outer diameter and 3-mm inner diameter requiring less than 50 μL of solution. Excitation of the sample was done through the bottom of the cell, and fluorescence was detected through the side wall of the cell at right angle. The cuvette was held in a copper cell holder which is temperature stabilized using a thermoelectric device based on thermoelectric coolers (ITI FerroTec Model 6300/035/085) and water/ethylene glycol bath. The emission was passed through a Glan Thompson polarizer and then a filter (optional). Then is was focused onto the entrance slit of a monochromator (Jobin-Yvon HR-250) whose output is focused either on the cathode of a fast photomultiplier tube (PMT, Phillips XP2020Q) with 800 ps FWHM of response function, or onto the cathode of a multianode microchannel plate photomultiplier (MA/MCP, Hamamatsu Corp., Japan).

The output of the PMT was sent to a constant-fraction discriminator (CFD, Tennelec 453), while the output of the MA/MCP was sent to a quad constant-fraction discriminator (CFD, Tennelec 454). The output of the CFD provided a start input for a time-to-amplitude converter (TAC, Tennelec 862) to which the stop pulse was provided by the cavity damper sync output. The TAC output was read by a combination analog-to-digital converter and multichannel analyzer (ADC/MCA, Nucleus PCA-II, 1024 or 8192 channels).

Experimental Procedure and Data Analysis. The reference lamp profile used for deconvolution of the experimental decay curve was obtained either from a scattered light pulse generated by placing a suspension of latex beads in the cell (when the MA/MCP was used) or by recording the decay curves of a reference compound under identical conditions (when the PMT was in use). The use and advantages of

reference compounds have been described before (Zuker et al., 1985; James et al., 1983). The reference compounds used were PBD/ethanol (τ = 1 ns, 360 nm) and POPOP/ethanol (τ = 1.37 ns, 475 nm), The reference solutions were freshly prepared for each experiment and checked for monoexponential decay. The linearity of the system response was routinely tested by measuring the decay curves of binaphthyl or anthracene which gave monoexponential decay curves. End-to-end distance distribution functions were derived from the experimental decay curves of the donor and the acceptor. Each distribution function was obtained by simultaneous global analysis of four experimental decay curves which were recorded under identical conditions. The fluorescence decay of the donor (excitation wavelength was 300 nm, emission at 360 nm with a bandwidth of 12 nm) was measured (a) in the absence of ET, obtained by measuring reference compounds of protein labeled by a single donor probe in the absence of an acceptor, and (b) in the presence of the acceptor at one of the specific sites. The fluorescence decay of the acceptor attached to a protein derivative (emission wavelength 475 nm with a bandwidth of 12 nm) was measured (c) without a donor (excited at 380 nm, using a flash lamp based time resolved fluorometer, a modified Edinburgh Instruments Model f-199) and (d) in a double-labeled protein derivative. A blank experiment was measured for each of the above decay curves, and the background was subtracted from each decay curve prior to the analysis.

Deconvolution and global analysis of the fluorescence decay curves were achieved using the Marquardt, nonlinear least-squares method (Beechem & Haas, 1989). The decay curves were fit to the solution of the second-order partial differential equation which takes into account both the energy-transfer perturbation term and diffusion between multiple conformations. The following equation was used for the cases in which the distributions of distances between probes had two subpopulations:

$$\frac{\partial p(r,t)}{\partial t} = D\frac{\partial}{\partial r}\left[\exp(-U(r)/k_BT)\frac{\partial}{\partial r}\exp(U(r)/k_BT)p(r,t)\right] - k(r)p(r,t) \quad (1)$$

In this equation $p(r,t)$ is the probability density to find an excited state donor with distance r from the acceptor at time t after excitation, D is the diffusion constant, and $U(r)$ is a distance-dependent potential of mean force in k_BT units (k_B, the Boltzmann constant; T, temperature). This potential is usually taken to be harmonic (thus implying a Gaussian distribution for the distance between the fluorescence probes): $U(r) = a(r - b)^2$, where a and b are parameters. $k(r)$ is the reaction term including the Förster energy-transfer rate and the spontaneous emission rate:

$$k(r) = -1/\tau_D[1 + (R_0/r)^6] \quad (2)$$

τ_D is the lifetime of the donor in the absence of an accpetor; R_0 is the Förster constant (i.e., the distance between the chromophores where transfer efficiency is 50%). R_0 was determined as previously described (Amir & Haas, 1987; Beals et al., 1991). Averaged energy-transfer efficiency was determined from the time resolved measurements using:

$$E = 1 - \frac{\tau_{DA}}{\tau_D} \qquad \tau_{DA} = \frac{\sum_{i=1}^{n}\alpha_i\tau_i}{\sum_{i=1}^{n}\alpha_i} \quad (3)$$

where α_i and τ_i are the amplitude and lifetime, respectively, of the ith component. τ_D and τ_{DA} are the donor lifetimes in the absence and in the presence of an acceptor.

RESULTS

The focus of the present work was to search for folding intermediate structures in reduced BPTI under partial folding conditions. Site specifically labeled protein derivatives were prepared, and the fluorescence decay of the donor and acceptor probes in the labeled BPTI derivatives was measured. Measurements were carried out under partial folding conditions, and the intramolecular end-to-end distance (EED) distributions were determined for each set of experimental conditions. Measurements were also made at low pH and at different salt concentrations.

The solvent composition for partial stabilization of the folding intermediates was selected according to the following considerations: (a) Only fully reduced BPTI was used, in order to observe the early folding intermediates. Therefore, DTT was included in each solution. (b) Low pH was used based on reports on stabilization of the MG state under acid conditions (A state) (Goto & Fink, 1990). (c) Low pH was also selected for solubility (and SNR) considerations. In neutral pH the solubility of reduced, unfolded, double-labeled BPTI derivatives is submicromolar, as determined by the intermolecular energy-transfer test. At this concentration, the background pulse height (at the peak) was more than 15% that of the pulse obtained when the fluorescence of the protein sample was monitored. This source of uncertainty sets the lower limit of the concentrations used for the samples. Due to this limiting uncertainty, determination of the intramolecular EED distributions in reduced BPTI derivatives, under standard folding conditions, was not possible in the present experiments.

In order to eliminate artifacts caused by microaggregations, due to the low solubility of unfolded BPTI, each series of experiments was preceded by a series of control experiments which tested for the absence of intermolecular energy transfer. Mixtures of donor labeled and acceptor labeled BPTI derivatives at a ratio of 1:1 were prepared. The fluorescence decay of the donor in those mixtures was measured for each solvent composition at a series of concentrations, and the limiting concentration for the onset of intermolecular energy transfer (ET) was determined. The experiments for determination of intramolecular ET in the double-labeled derivatives were carried out using protein concentrations lower than the limits determined in these control experiments. Acid pHs were used in order to avoid microaggregations at the concentration levels required by the SNR (1−2 μM protein concentrations).

The fluorescence decay curves of labeled derivatives were measured under the following partial folding conditions: (A) "R state": "Partially folding" conditions in 0.5 M GuHCl, 50 mM format buffer pH 3.6, and 5 mM DTT. (B) "A1 state": Acidic conditions in 0.5 M GuHCl, 50 mM glycine

Table 1: Transfer Efficiencies[a] in Reduced BPTI Derivatives in the U, R, and A1 States

	R state				A1 state		U state[b]	N state[c]
deriv[d]	2 °C	20 °C	35 °C	60 °C	2 °C	20 °C	20 °C	20 °C
1−15	57 ± 3	65 ± 4	58 ± 5	58 ± 11	75 ± 2	77 ± 5	53 ± 3	44 ± 5
1−26	53 ± 4	57 ± 3	64 ± 4	66 ± 2	53 ± 8	63 ± 6	35 ± 2	84 ± 5
1−41	72 ± 5	73 ± 3	71 ± 8	60 ± 2	39 ± 3	49 ± 11	28 ± 1	85 ± 5
1−46	57 ± 6	66 ± 5	60 ± 5	57 ± 2	60 ± 6	56 ± 5	28 ± 1	80 ± 5

[a] Average transfer efficiencies in percent. [b] Taken from Gottfried & Haas, 1992. [c] Taken from Amir and Haas, 1987. [d] (1−*n*)BPTI.

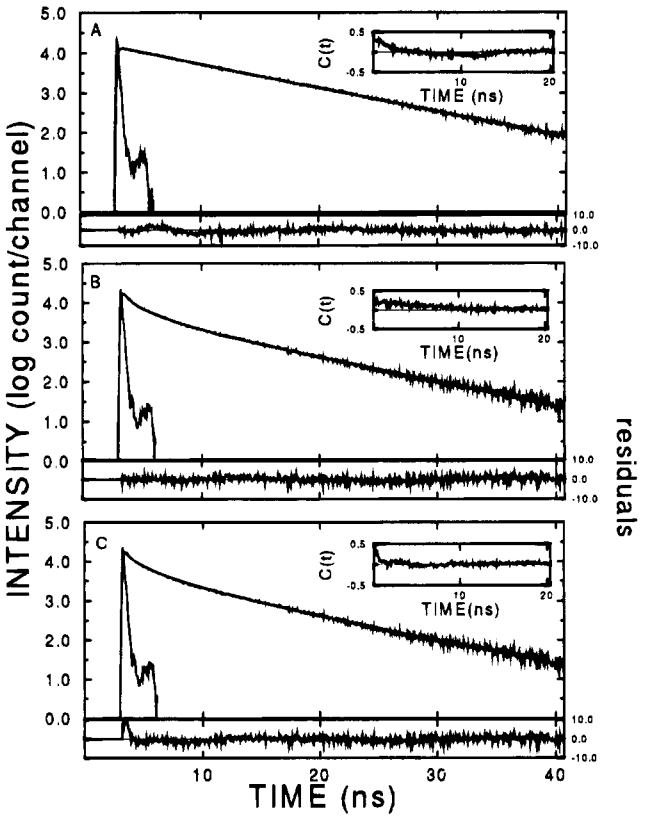

FIGURE 2: The florescence decay of MNA, the donor, attached to the N-terminal residue of BPTI derivatives in the R state, in 0.5 M GuHCl, 50 mM formate buffer, pH 3.6, and 5 mM DTT at 20 °C. The excitation wavelength was 300 nm, and the emission was measured at 360 nm, bandwidth 20 nm. (A) A derivative that has no acceptor, the decay of the donor was close to monoexponential with $\tau_1 = 6.2$ ns, $\tau_2 = 1.55$ ns, $\alpha_1 = 0.95$, and $\alpha_2 = 0.05$, $\chi^2 = 1.76$. (B) An exponential analysis of the donor emission in the double-labeled derivative (1-26)BPTI, in which the acceptor was attached to Lys-26 at the ϵ-amino group. Three exponential components were included. The average lifetime was 1.72 ns and $\chi^2 = 1.89$. (C) Same sample and experiment as in (B) analyzed for EED distribution using the global analysis. The best fit parapmeters are given in Table 2, the local $\chi^2 = 2.7$.

buffer, pH 2.1, and 5 mM DTT. (C) "A2 state": Desalted acidic conditions in 50 mM glycine buffer, pH 2.1, and 20 mM DTT.

Average Transfer Efficiencies. The fluorescence decay curves of the donor (MNA) attached to the N terminus of the protein in the MNA-BPTI derivative (no acceptor) was close to monoexponential under most conditions tested here (with small very short component is some experiments, ca. 5%) (Figure 2A). The same measurements applied to the double-labeled derivatives, (1−*n*)BPTI, under the partially folding conditions (R state) yielded multiexponential decay curves. At least three components are needed for an acceptable fit of the data (Figure 2B). The deviations from monoexponential decays are a manifestation of the multiplicity of conformations (intramolecular distances) *and* of the time dependence of the distances due to fast conformational fluctuations. Figure 2C shows the same set of data shown in Figure 2B, analyzed by the global analysis for EED distributions.

The results shown in Table 1 show that *the dependence of transfer efficiency on segment length is small.* All derivatives in the series, which span a range of segment lengths from 15 to 46 residues (3-fold), yielded transfer efficiencies around 60%. The transfer efficiency obtained for the (1−41)BPTI was higher; at low temperatures it was about 70%. This shows that, under partial folding conditions in low GuHCl concentration, *reduced BPTI is in a compact state, but this state is not a condensed statistical coil conformation.* Any statistical ensemble of condensed conformations would have yielded decreasing transfer efficiencies as a function of chain segment lengths.

The transfer efficiency obtained for the 41 residue segment, which was higher than that found for the 15 and 26 residue segments, is another indication that the conformation of BPTI in this compact state is characterized by an ensemble of nonrandomly folded conformations. The detailed analysis presented in the next section shows that this state is even more complicated.

Table 1 also shows that the compact state stabilized under partial folding conditions is also characterized by a *weak temperature dependence* of the transfer efficiencies, i.e., of the intramolecular distances. This is in sharp contrast to the dependence observed for the same derivatives in 6 M GuHCl (the U state) (Gottfried & Haas, 1992). No reversible cold unfolding could be observed in the present experiments. This shows that, under partial folding conditions, the BPTI molecule is folded in a loosely stabilized conformation, which does not have a cooperative temperature dependent conformational transition in the temperature range between 2 and 60 °C.

The average transfer efficiencies shown in Table 1 for the 26, 41, and 46 residue segments are between 75% and 85% of those found for oxidized BPTI in the native state (Amir & Haas, 1987). A clear exception to this is the transfer efficiency monitored within the N-terminal segment using (1−15)BPTI. The average transfer efficiency within this segment in the R state is ca. 60%, considerably higher than the values observed in the native state. Clearly this segment is folded into a more compact conformation in the R state. Details of the conformational transitions are revealed by global analysis of the fluorescence decay curves of both the donor and acceptor probes.

Determination of Distance Distributions: The EED Distribution Functions under Partial Unfolding Conditions. The results of the distance distribution analyses are shown in Table 2. As was already found in previous experiments (Gottfried & Haas, 1992), a model consisting of at least two subpopulations of the segmental EED distribution was required for the analyses of the decay curves. The procedure

Table 2: Parameters of the Segmental End to End Distance Distributions of the BPTI Derivatives in the R-State

deriv[a]	T[b] (°C)	R_{av1}[c]	W_1[d]	R_{av2}[e]	W_2[f]	frx[g]	diff[h]	χ^2, single[i]	χ^2, double[j]
1−15	2	22.7 (21.4−23.6)	2.6 (2.6−4.7)	35.6	3.1	0.65 (0.60−0.80)	0.002 (0−2)	6.26	2.99
	20	21.5 (20.5−22.9)	3.8 (3.1−4.7)	35.6	3.1	0.78 (0.72−0.78)	0.015 (<2)	4.21	3.35
	35	21.2 (20.3−22.4)	2.4 (2.1−3.9)	35.6	3.1	0.65 (0.60−0.70)	0.005 (0−2)	15.02	6.52
	60	21.5 (20.3−22.4)	2.2 (2.1−2.6)	35.6	3.1	0.72 (0.70−0.75)	0.013 (0−3)	14.20	5.06
1−26	2	20.4 (18.9−22.2)	5.2 (3.6−7.0)	53.8	9.6	0.61 (0.50−0.75)	0	26.00	4.45
	20	18.6 (17.0−21.1)	5.4 (3.4−6.9)	44.7	9.4	0.66 (0.55−0.75)	5.7 (4−9)	5.46	3.72
	35	20.4 (18.2−21.3)	4.2 (3.4−5.2)	53.8	9.6	0.81 (0.75−0.85)	0.8 (0−8)	29.06	5.24
	60	20.8 (19.7−21.5)	2.5 (2.3−4.7)	53.8	9.6	0.77 (0.70−0.80)	0.6 (0−2)	15.20	9.44
1−41	2	16.2 (16.0−16.7)	6.7 (5.1−7.1)	53.8	9.6	0.93 (0.93−1.0)	2.8 (0−5)	10.40	3.45
	20	18.7 (18.1−19.2)	5.9 (5.2−7.5)	53.8	9.6	0.91 (0.90−0.98)	0.92	6.86	3.55
	35	19.0 (17.5−21.1)	6.0 (4.2−7.9)	53.8	9.6	0.83 (0.75−0.85)	2.5 (0−18)	10.72	5.98
	60	22.0 (20.8−23.0)	3.1 (2.8−3.4)	53.8	9.6	0.72 (0.65−0.75)	0 (0−14)	10.01	7.06
1−46	2	20.7 (20.2−21.0)	4.7 (3.9−6.2)	44.7	9.5	0.77 (0.75−0.80)	0.57	5.59	3.33
	20	21.1 (20.8−21.5)	5.1 (3.9−6.3)	53.8	9.6	0.85 (0.80−0.85)	0.104	6.65	4.40
	35	23.0 (21.8−23.1)	3.6 (2.5−3.9)	53.8	9.6	0.77 (0.65−0.80)	0 (0−20)	9.80	3.65
	60	22.8 (21.3−23.4)	2.33 (2.3−4.3)	53.8	9.6	0.75 (0.70−0.80)	0.27 (0−4)	7.39	4.25

[a] (1−*n*)BPTI derivatives; values in parentheses are confidence intervals determined by rigorous analysis. [b] Temperature. [c] Maximum of the first subpopulation EED, in Å. [d] Width of the first subpopulation EED (standard deviation), in Å. [e] Maximum of the second subpopulation EED, in Å. [f] Width of the second subpopulation EED, in Å. [g] Fraction of the first subpopulation. [h] Intramolecular diffusion coefficient 10^{-7} cm^2/s. [i] χ^2 obtained by global analysis assuming single EED distribution. [j] χ^2 obtained by global analysis assuming two EED distribution.

of adding a second distance distribution was used. The second distribution, with a fixed peak distance and width parameters, was determined empirically by a grid search. Although this improved the goodness of fit in most cases, some experiments could not be perfectly fit even with this expanded model. In those cases the bimodal distributions improved the fit of the experimental decay curves but were only a good approximation for the actual distributions. The second distribution which was required for the best fit was found to include very long interprobe distances corresponding to an expanded conformation of the protein backbone. Thus, under the conditions used here, *the conformation of labeled BPTI derivatives was found to be an equilibrium mixture of at least two conformational subpopulations. One subpopulation was usually found to be in a fully unfolded conformation.*

The parameters of the segmental EED distributions in the R, A1, and A2 states are listed in Tables 2 and 3. The calculated segmental EED distributions are shown in Figure 3A−D. In most of the experiments the dominant subpopulations of the conformers were the compact native-like subpopulations.

When separations between the donor and acceptor are greater than approximately $1.6R_0$, the transfer efficiencies are low and the uncertainty intervals are large. This was the case in the range of distances larger than ca. 45 Å, corresponding to the major portion of the extended subpopulations. Therefore, the shapes of the EED distributions of the expanded subpopulation presented in Figures 3 and 4 are first order approximations only. The meaning of the analyses for these expanded subpopulations was that a corresponding portion of the molecules had an extended EED, larger than 40 Å.

The two subpopulations appear to be in equilibrium, which is affected by temperature (weakly) and by solvent composition. Interestingly, the main effect of temperature changes, in most cases, was *a change in the ratio between the two subpopulations*, i.e., a transition of a fraction of the unfolded subpopulation to the compact subpopulation. In the discussion of the EED distributions below, the terms α, β, and γ were used not in the sense of secondary structures, which apparently do not exist in the conditions used here, but rather as names for chain segments 1−11, 21−30, and 46−58, respectively, regardless of their structure under any specific partially folding conditions.

The N-Terminal Segment, (1−15)BPTI. The EED distributions within the N-terminal segment monitored in (1−15)BPTI are shown in Figure 3A. Three effects are of interest: (1) The main subpopulation (the folded fraction 0.78 in the R state and 0.87 in the A1 state) had a mean segment length of 20−25 Å, considerably *smaller than the length found in the native state.* (2) The minor subpopulation had an expanded native-like conformation (with a mean EED close to that of the native state (ca. 32 Å (Amir & Haas, 1987)). This subpopulation, which was maximal in the R state, was decreased in the A state (like in the U state). (3) Reduction of the GuHCl concentration and the pH caused a further *contraction of the N-terminal segment.*

These results show that, in the absence of cross links contributed by disulfide bonds (probably the 14−38 disul-

Table 3: Parameters of the Segmental EED Distribution of the Labeled BPTI Derivatives in the A1 and A2 States

state	deriv[a]	T[b] (°C)	R_{av1}[c]	W_1[d]	R_{av2}[e]	W_2[f]	frx[g]	diff[h]	χ^2, single[i]	χ^2, double[j]
A1	1−15	2	19.2	4.4	35.6	3.1	0.93	0	2.63	2.05
			(15.8−20.2)	(2.9−5.9)			(0.90−0.95)	(0−4)		
		20	21.6	2.9	35.6	3.1	0.87	0.05	7.16	2.27
			(20.7−23.5)	(2.6−3.9)			(0.80−0.95)	(<2)		
	1−26	2	20.8	8.2	53.7	9.6	0.76	0	14.9	2.13
			(19.6−22.4)	(3.9−16.6)			(0.60−0.85)	(0−2)		
		20	24.5	2.3	53.7	9.6	0.53	26	7.75	2.53
			(23.5−26.3)	(2.2−6.0)			(0.50−0.70)	(20−28)		
	1−41	2	30.2	4.1	53.7	9.6	0.39	0.13	16.9	1.95
			(27.9−32.9)	(2.4−4.8)			(0.25−0.45)	(<12)		
		20	27.8	2.9	53.7	9.6	0.42	23.8	6.82	2.58
			(26.1−28.8)	(2.5−3.7)			(0.35−0.45)	(18−30)		
	1−46	2	27.0	3.6	53.7	9.6	0.70	0.04	20.2	3.20
			(25.7−30.4)	(2.3−4.7)			(0.55−0.75)	(0−16)		
		20	25.8	2.2	53.7	9.6	0.61	≅0	13.0	3.50
			(24.6−28.4)	(1.8−4.3)			(0.55−0.65)			
A2	1−41	20	25.4	4.0	53.7	9.6	0.60	0.17	5.49	4.44
			(24.6−26.3)	(2.5−5.3)			(0.50−0.65)	(0−14)		
	1−46	2	24.3	3.6	53.7	9.6	0.60	27.5	7.93	2.35
			(20.9−26.8)	(27.2−6.1)			(0.55−0.70)			
		20	22.6	4.2	53.7	9.6	0.72	0.07	6.88	3.24
			(20.6−23.7)	(3.4−5.2)			(0.65−0.75)	(0−6)		

[a] (1−n)BPTI derivatives; values in parentheses are confidence intervals determined by rigorous analysis. [b] Temperature. [c] Maximum of the first subpopulation EED, in Å. [d] Width of the first subpopulation EED (standard deviation), in Å. [e] Maximum of the second subpopulation EED, in Å. [f] Width of the second subpopulation EED, in Å. [g] Fraction of the first subpopulation. [h] Intramolecular diffusion coefficient 10^{-7} cm^2/s. [i] χ^2 obtained by global analysis assuming single EED distribution. [j] χ^2 obtained by global analysis assuming two EED distribution.

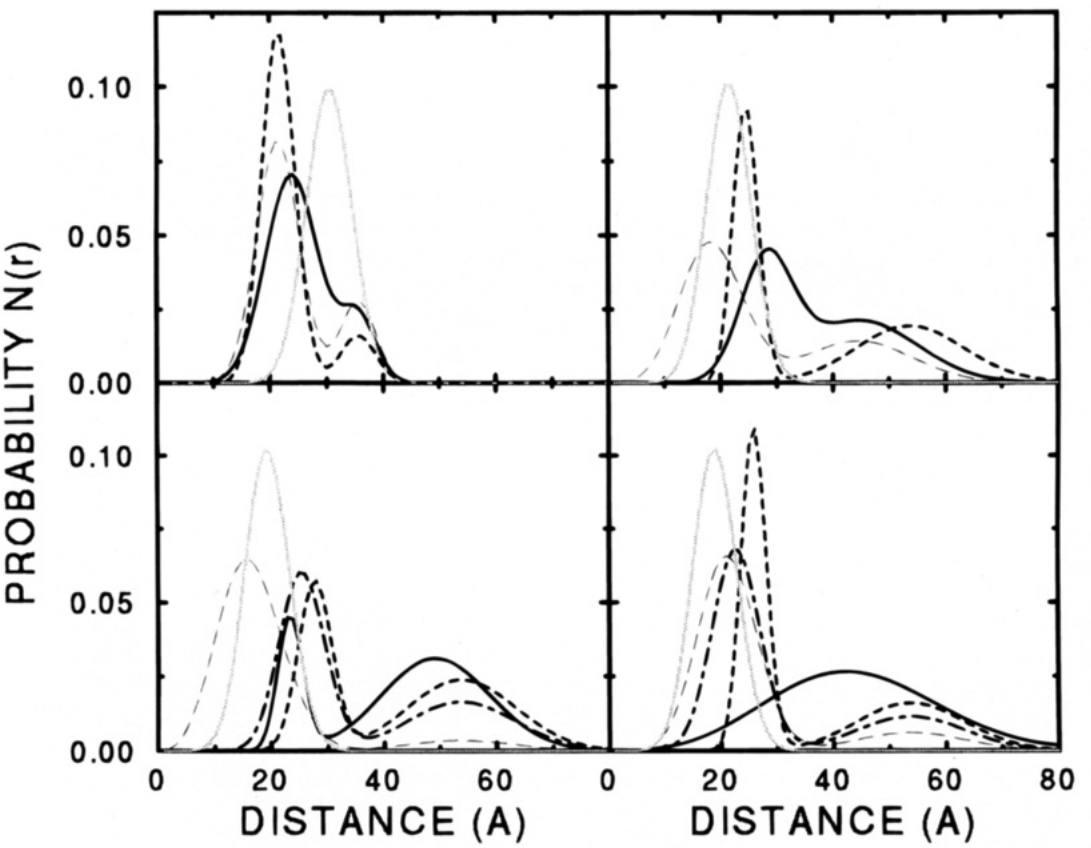

FIGURE 3: The EED distributions of the four BPTI derivatives in the U state (—), the R state (— — —), the A1 state (- - -), and the A2 state (— - —). The faint dotted trace marks the native EED distribution for each derivative. The derivatives are (A) (1-15)BPTI, (B) (1-26)-BPTI, (C) (1-41)BPTI, and (D) (1-46)BPTI.

fide), the N-terminal segment of BPTI, which is relaxed into a statistical coil conformation under unfolding conditions (Gottfried & Haas, 1992), did not form the native conformation and maintained even slightly more relaxed *non-native-like conformation* in the R and A states.

This is apparently stabilized by nonlocal interactions (including hydrophobic interactions) with the hydrophobic core of the protein. As a result of this relaxation and possible stabilizing interaction under these conditions, there exists a subpopulation of BPTI molecules which are compact, and their structure is more *spherical* (globular) than the oblate structure of the molecule in the native state. A possible structural interpretation of this observation is that the flexible N loop (residues 12−18) is "collapsed" on the hydrophobic

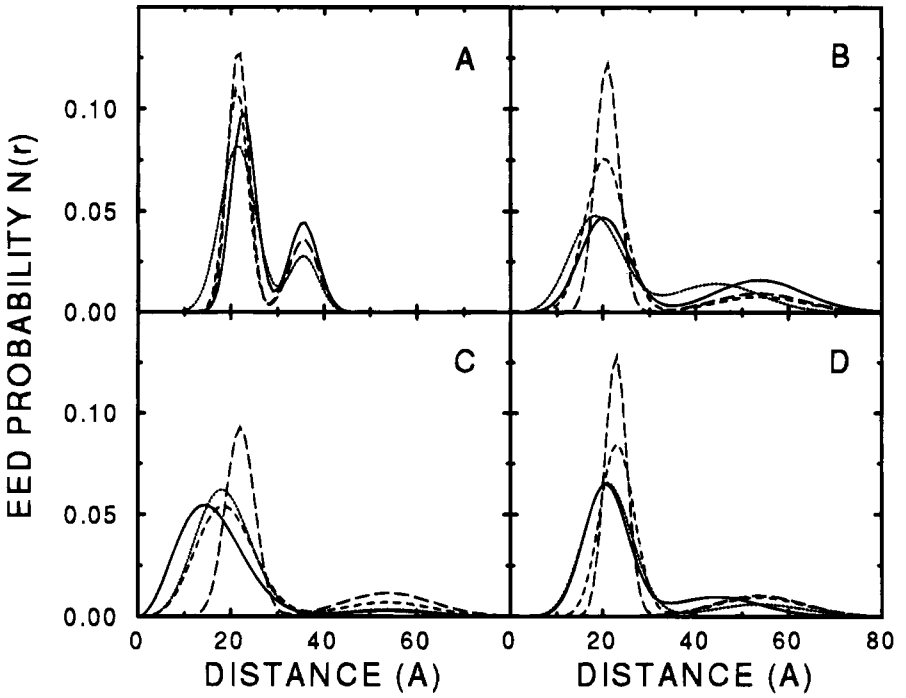

FIGURE 4: The temperature effect on the segmental EED distributions in reduced BPTI in the R state: (—) 2 °C, (•••) 20 °C, (- - -) 35 °C, (— —) 60 °C. The derivatives are (A) (1-15)BPTI, (B) (1-26)BPTI, (C) (1-41)BPTI, and (D) (1-46)BPTI.

core of the molecule in which the terminal segments are held by specific interactions. A question of interest at this point is whether the native oblate shape can be stabilized in BPTI without the cross link contributed by the 14−38 disulfide bond, which has been shown to be under extra strain (Van Mierlo et al., 1991). This is equivalent to the question whether the β structure can be stabilized in its native structure in the reduced state. It has been suggested that the N-terminal segment is unfolded in the partially reduced state (Van Mierlo et al., 1991).

The 26 Residue Segment (1−26)BPTI. Figure 3B shows changes in the EED distribution between residues 1 and 26 in response to dilution of the denaturant and lowering of the pH: The change of the relative size of the two subpopulations in response to the transition to the R and A states was very moderate. The change in the transfer efficiencies was accounted mainly by shifts of the means of the short EED subpopulation and perhaps to some extent by increased dynamic flexibility (R state at 20 °C, Table 2).

It is pertinent to note that in the unfolding and partially folding conditions studied here no evidence for secondary structures in BPTI was found (Gussakovsky & Haas, 1991; Lumb & Kim, 1994), and therefore, the β structure may not be formed. The N-terminal segment, residues 1−15, is not in a native length and seems to be relaxed to an EED shorter than the native one. Therefore, the native interactions between the native secondary structures (formed in γ and β) within this 26 residue segment are unlikely to be effective. The bias of the 1−26 EED distribution toward the native-like position (Figure 3B) is apparently stabilized *both by the hydrophobic collapse and by specific NLIs between the two termini of this segment* which are held in close proximity despite the unfolded state of the 1−15 segment and the β strand from 16 to 27.

The 41 Residue Segment, (1−41)BPTI. Figure 3C shows the dependence of the EED distribution between residues 1 and 41 in reduced BPTI on the concentration of the denaturant. In the U state, in 6 M GuHCl, the average transfer efficiency was the lowest found in the present series of derivatives. The analysis showed that 60−80% of the molecular population was in the unfolded subpopulation. When the reduced (1−41)BPTI was transferred to a low GuHCl concentration, the transfer efficiency was higher than that of any other derivative. The global analysis showed that this was the combined effect of two changes: (1) *a major increase of the short EED subpopulation, from 20−40% to 90%* (conformers with native-like segmental 1−41 EED), and (2) concomitant compaction of the native-like subpopulation, shown by a shift of the peak of its EED distribution (Figure 3C). Further reduction of the pH to 2.1 induced an acid unfolding which is shown both by the increase in the size of the unfolded subpopulation and by a shift of the mean of the native-like subpopulation to longer EED.

These results show that the 41 residue segment (1−41) is the least folded segment in reduced BPTI under unfolding (U) conditions and undergoes the *largest change* when the GuHCL concentration is decreased. Residue 41 is located on the C-terminal loop of BPTI (Figure 1) but close to C terminal segment, which is found to be in strong interaction with the N-terminal and the central (β) segments. The larger local changes in the 1−41 EED distributions can be interpreted as the combined effect of the NLIs between the chain termini and the hydrophobic collapse. Specifically, this includes the NLI between the chain termini (or between the C terminus and the β segment), local interactions of the minor β element (residues 44−45) with both α and β, and hydrophobic interactions of the loop residues (38−43) with the hydrophobic core of the molecule. (This last interaction of the flexible section of the loop can be similar to that found in the N-terminal loop discussed above.)

The 46 Residue Segment, (1−46)BPTI. Transition from the U state to the R state at room temperature was accompanied by a major contraction of the 1−46 segmental distance (Figure 3D). The subpopulation with a native-like 1−46 EED, which had an average distance of 21 Å, comprised of 85% of the total population. This means that,

in the major fraction of the molecules, the distance between the chain termini was close to that found in the folded state. Thus in the R state the 1−46 segmental EED looks very much like in the N state. The structures of the conformers in the major subpopulation, like that with the native-like 1−46 segmental EED, are probably stabilized by specific NLIs between the α segment and the γ and β segments. It is conceivable that the same NLIs are effective in the N state, in which the chain termini are in close proximity. The size of this subpopulation was similar to that found for the 41 residue segment in the R state.

Transition to lower pH, the A1 state, causes an increase in the subpopulation with the extended EEDs as was also found when the 1−41 EED was monitored. This decrease in the fraction of molecules with a short average 1−46 distance was only 50% that found in the 1−41 derivative. It seems reasonable to assume that this is a result of the hydrophobic interactions between the α, β, and γ segments. This conclusion is further supported by the experiment which shows that, in this derivative, desalting at low pH (A2 state) did not change the percentage of the two subpopulations (Figure 3D).

The results presented in Figure 3 also show that the EEDs of the medium length segments (26 and 41 residues) show stronger dependence on the pH. This is another indication that the terminal segments are held in stronger interactions, probably hydrophobic, even under partially folding conditions.

The Effect of Temperature on the Intramolecular Segmental EEDs. Global analysis of the decay curves shows the fine details of the temperature dependence (Figure 4). The effect is small, and the only parameter in which marginally statistically significant dependence can be observed (according to the rigorous statistical analysis shown in Tables 2 and 3) is the population ratio ("frx" in the tables) in the 26 and 41 residues segments, albeit only very weakly.

In the 41 residue segment, at the higher temperatures there is an increase of the unfolded subpopulation and also a shift of the peak of the EED distribution of the compact subpopulation toward larger distances. At the higher temperatures the proportion of the compact subpopulation was decreased from 0.93 (0.93−1.0) at 2 °C, to 0.72 (0.65−0.75) at 60 °C.

The distance between residues 1 and 46 also shows greater stability than that of the shorter 1−41 residues segment. Unlike the cold unfolding found for the whole chain in the U state, the temperature dependent changes are limited in the R state (decreased width of the short EED subpopulation). This is probably the contribution of the α−β and α−γ interactions (the α−γ interaction can be mediated by the interactions of α and γ with both sides of β). It appears that the change is small due to the stability contributed by the interactions of the terminal segments and that the thermal unfolding is counterbalanced by hydrophobic stabilization.

DISCUSSION

The main goal of the present work was to determine the role of NLIs in the stabilization of subdomain and local folding transitions and to detect the formation of the overall topology in the partially folded states of BPTI. The partial folding conditions can be considered as stabilizing subdomain structures which may be populated in the early folding intermediates of the protein. This is based on the approximation (or postulate) that since the control of the folding pathway is under both thermodynamic and kinetic control (Uversky et al., 1992), one can simulate features of a folding pathway by a sequential removal of the unfolding agents and progress along the "stabilization coordinate" (Shortle, 1993). The implicit assumption is made that structural elements with larger internal stability can also function as chain folding initiation structures (CFIS; Monetlione & Scheraga, 1989) and appear earlier on the time dependent pathway. In the initial folding intermediates, or more stable subdomain structures, there appear to be the contribution of local interactions and hydrophobic collapse driven by solvent exclusion. In the destabilizing conditions studied in the present work, BPTI was in a reduced state (no disulfide cross links), and no secondary structures were found under the conditions used here (Gussakovsky & Haas, 1992; Lumb & Kim, 1994). Yet a *compact conformation* was assumed by the protein. The EED distributions found in the present experiments show (a) that the average compact structure is in fact an equilibrium of two (or more) subpopulations and (b) that this is *not a collapse into a statistical coil conformation*. The short EED subpopulations of the longer segments (26, 41, and 46 residues) show that *a native-like topology is formed in the partially folded states* which is directed and partially stabilized by specific NLIs (in addition to the other stabilizing interactions mentioned above). In order to evaluate the significance of the results, we shall first discuss the experimental conditions and then the conclusions.

Experimental Conditions and Control Experiments. The single photon counting method allows for long averaging time and accumulation of very low signals. Yet, the actual limit is set by the background signal which cannot be reduced by long averaging time. Therefore, no measurements at neutral pH (folding conditions with reduced protein) were performed in order to ensure both full solubility and acceptable SNR.

A control for absence of intermolecular energy transfer in the experimental setup (defined by the concentrations, solubility of the derivatives, temperatures, and solvents) was made by measuring the donor fluorescence decay and excitation spectra of a mixture of $(MNA)_2$-BPTI and $(DA\text{-}coum)_2$-BPTI (at a ratio of 1:1). The concentrations of BPTI derivatives used were in the range of 1−2 μM (the limit set by the background fluorescence); no intermolecular energy transfer was detected under the above conditions. This control experiment rules out intermolecular energy transfer due to aggregations or short average intermolecular distances. It should be noted that this control is very sensitive to any degree of aggregation. No turbidity could be visible in solutions which showed intermolecular energy transfer. This is an advantage of the fluorescence methods which can be used at micromolar concentrations, which is essential for conformational studies of reduced partially unfolded states of proteins in solution.

The analysis is based on a model of long range nonradiative excitation energy transfer between the probes. The obvious question is whether additional de-excitation mechanisms could not affect the photophysics of the probes and be misinterpreted as conformational changes. It is not possible to eliminate all uncertainties; however, most of the questions were discussed in previous publications based on the present model compounds. These will not be repeated here except for the questions specifically relevant to the

conditions used in the present experiments. The series of control experiments described below was made, which reduce the probability of misinterpretation of the physical measurements.

The interpretation of the results presented in the present work is based on the chemical and spectral characterizations of the labeled derivatives published earlier (Amir & Haas, 1987, 1988; Amir et al., 1992; Gottfried & Haas, 1992). The main questions are whether the exposure of hydrophobic surfaces in the low GuHCl concentrations or change of protonation states of the protein can allow direct interaction between the dyes or between the dyes and the protein backbone or side chains, in a manner that can change the transfer efficiencies.

The conclusions are based on global analysis of the fluorescence decay kinetics of both the donor and the acceptor of the excitation energy (Haas et al., 1978a; Beechem & Haas, 1989). The essential control experiments and possible errors (e.g., the orientation problem) were already previously discussed in detail with regard to the set of derivatives used here and therefore will not be repeated. A few additional control experiments and possible uncertainties of the experimental and computational procedures will be discussed below, followed by a discussion of the significance of the observations.

The design of the experiments was based on labeling solvent exposed side chains. This allows full solvation of the probes and thus minimization of possible direct interactions of the probes with hydrophobic sites in the partially folded protein or restriction of the orientational averaging. The lack of such possible interactions of the probes was routinely checked by measurements of the emission spectra of the probes and the steady state polarization. No shifts of the emission maxima relative to those of the probes in each solvent were observed (indeed, the MNA emission is environmentally insensitive, but the coumarin emission spectrum is known to be blue shifted in nonpolar or dynamically restricted sites). Thus the changes of transfer efficiencies cannot be attributed to changes in the orientations of the probes or changes of spectral parameters (e.g., overlap) induced by interactions. The probes themselves reported normal solvation under all conditions used here, and the interpretation based on changes of the distances' distributions is valid.

Spectroscopic Considerations. The analyses of the time resolved energy transfer measurements depend strongly on two parameters, τ_D, the donor fluorescence decay constant in the absence of an acceptor, and R_0, the Förster constant. τ_D was measured in each experiment using MNA-BPTI, a donor only BPTI derivative attached at the same site as in the double-labeled derivatives. The decay of the fluorescence of MNA-BPTI was close to monoexponential under most of the experimental conditions employed in the present study, and thus all the specific effects induced by the changing conditions (e.g., temperatures, solvent components, and instrumental parameters) were automatically taken into account. By inclusion of these reference experiments in the global analysis without prior processing, no assumptions, corrections, or approximations had to be made.

R_0 was calculated using experimentally determined refractive indices, donor quantum yields, and acceptor absorption and donor emission spectra. Thus, changes in transfer efficiencies due to molecular and spectroscopic effects of solvents and temperatures were also taken into account by their effect on R_0.

The question whether alternative de-excitation mechanisms due to specific local interactions in any of the derivatives took place was addressed by monitoring simultaneously the donor and the acceptor emissions. Steady state excitation spectra confirmed that the quanta which were subtracted from the donor emission did show up in the acceptor emission. The global analysis also took into account the acceptor decay curves.

An extreme case of direct contact of the probes is also very improbable. In such a case the very short component of the donor lifetime can be missed, but the increase in acceptor emission intensity and the probable shift in the acceptor emission wavelength should show up. No such discrepancy was found. Even if a minor subpopulation does have perturbed conformation in one of the states, this should not reduce the significance of the conclusions reported here, since the main parameters of the EED distributions are anyway not very sensitive to the edges of the distributions.

A frequently cited potential source of uncertainty in the magnitude of R_0 is the dependence of transfer probabilities on the orientations of the probes. Two uncertainties are involved: (1) the possible contribution of distributions of orientations to the observed distribution of transfer efficiencies and (2) the question of the correct average R_0 for each derivative. This issue has been discussed in detail by many authors (Jones, 1970; Hillel et al., 1976; Haas et al., 1978b; Stryer, 1978; Dale et al., 1979). A detailed discussion of theoretical and experimental considerations has been presented (Amir & Haas, 1987; Gottfried & Haas, 1992), leading to the conclusion that the probability for a value of R_0 differing by more than 10% from the dynamically averaged R_0 ($\kappa^2 = {}^2/_3$) is small (Haas et al., 1978b). In a previous work (Amir et al., 1992) it was shown that even in viscous solutions the averaging of the orientations is effective. The high temperatures and low viscosity of the solutions used in all the experiments reported here further reduce the uncertainties due to the orientation effect.

Considerations Pertaining to the Data Analysis: The Significance of the Bimodal EED Distributions and the Quality of Fits. The limiting factor in analysis of fluorescence decay curves is the correlation between the calculated free parameters. In order to reduce the number of free parameters and thus reduce the statistical uncertainty, model functions were used for the EED distributions and the fluctuations. The model introduced constraints which enabled the determination of its parameters within reasonable error ranges. The ranges of acceptable values were determined for each parameter by rigorous error analysis (Beechem & Haas, 1989). The χ^2 values are given in Table 2. In some experiments the best fits obtained using the present model function were high, but the differences between the lowest χ^2 values obtained for single or two subpopulations models were large enough to reject the first model.

The evaluation of each analysis and significance of the parameters was based on the χ^2 values, the distributions of the residuals, the autocorrelation of the residuals, and the error intervals of the calculated parameters (Grinvald & Steinberg, 1974). The error intervals were determined by a rigorous analysis (Beechem & Haas, 1989).

All the experiments done under partial folding conditions were fitted to distributions consisting of two subpopulations. A fit to a single component distribution gave a skewed

distribution with increased χ^2. Repeated analysis assuming two component EED distributions gave the results shown in Figures 3 and 4. The improvement of fit gained by the inclusion of the second subpopulation was significant, as judged by the reduced χ^2 and distributions of the residuals. Yet, in most experiments the quality of the fit to the bimodal EED distribution was not close to the commonly accepted value of $\chi^2 = 1$. The question is why, and what is the significance of the shapes of the EED distributions presented in Tables 2 and 3 and Figures 3 and 4. This is discussed below, but first it should be born in mind that the same BPTI derivatives in the native state, even in 6 M GuHCl (nonreduced disulfides), gave single component EED distributions (Amir & Haas, 1987). The observation that there are two subpopulations is not an artifact of the experimental setup.

The high χ^2 values and the autocorrelations of the residuals (in some experiments) reflect systematic differences between the experimental decay curves and the calculated curves based on the model selected for the analysis. The deviations are of two categories:

(a) Nonrandom noise such as nonlinearity of the instrument response (e.g., the linearity of the time to amplitude converter (TAC)) or background fluorescence. The linearity of the instrument response was routinely tested by measurements of standard materials with known monoexponential decay. In some periods the system showed systematic oscillations which did not affect the parameters which gave the best fit, except for the increased χ^2 values. The background emission was routinely measured for each experiment and subtracted from the data before the analysis. As mentioned above, the limited solubility of the reduced protein derivatives dictated measurements at the lowest possible concentrations. The background emission was kept in the limit of 15% at the peak emission. Small errors in the subtraction could also be source of nonrandom noise that increased the χ^2 values of the best fit, regardless of the adequacy of the model.

(b) The second source of systematic deviation is the limited flexibility of the model used for the reconvolution. That means that the conformational distributions and the dynamics are more complex than the simple description of the current model and, perhaps, that the analysis does not recover all the details of the EED distributions. Yet, due to limitations in the number of parameters, the simpler models were used. In principle, this means that more information could be extracted from the data, provided that additional overdetermination would be contributed by additional experiments. Measurements of the same EED distributions using pairs of dyes with larger or smaller R_0, or determination of the transfer anisotropy decay (Chen et al., 1992), are possible improvements. Possible causes for the lack of perfect fit are the following: additional conformational subpopulations in the unfolded chains, an asymmetric shape of the EED distributions, and distance dependence diffusion coefficients. Length dependent intramolecular diffusion coefficients can be found for conformers in which the ends of the labeled segments are under the effect of an NLI within the segment, or with other parts of the chain. These are less flexible than the conformers in the second subpopulation. It is possible that the dynamics of some chain segments is not a simple stochastic process and therefore the Fick type model (eq 1) cannot give a perfect fit. In principle, it is possible to add such features into the model function used in the analysis. But every parameter added would increase the correlation between the parameters and reduce the statistical significance. Therefore, the analyses were carried out using the simpler model, which gave good approximations of the EED distributions at the expense of the high χ^2 values. Even in the current level of simplication of the model function, the parameters characterizing the EED distribution, the means of the distribution, and to a lesser extent, the widths are very well recovered.

Simulations were used to give an estimation of the differences in the criteria for the quality of fit of a decay curve generated by a bimodal EED distribution when analyzed by models of single or two subpopulations. Decay curves were simulated using two component EED distributions, and experimental noise was added to the simulated curves. The differences in the χ^2 values which were obtained by the addition of the second subpopulation in the analyses were statistically significant. For instance, analysis of one of the simulated decay curves gave χ^2 values of 2.56 and 3.00 for double and single component EED distributions, respectively. This shows that the differences in the χ^2 values found in Tables 2 and 3 are significant and reflect differentiation between the two models. For the present discussion the main conclusion is that, under partially folding conditions, at low pH, the segmental EED distributions studied here in reduced BPTI have high populations of the short distances which correspond to a folded conformation.

The error ranges (which were obtained by rigorous analysis procedures) presented in Table 2 show that the significance of the means of the EED distributions and the corresponding widths are quite high. The main uncertainties are as follows: (1) For the samples used in the present experiments the donor lifetime is only weakly distance dependent at distances larger than 45 Å. At distances shorter than ca. 16 Å the donor lifetime is very short. Therefore, all conformers with EEDs smaller than the lower limit have the same contributions to the transfer efficiency. Those with EED in excess of 45 Å have no contributions to the ET. The shape of the EED distributions is significantly determined only in the range of 16−45 Å in the present system. The curves shown in Figures 3 and 4 outside these boundaries are due to the model used and can assume any other shape as the analysis cannot discriminate the shapes. The analysis does give the results of the integrated size of the population of conformers which have EEDs above or below the corresponding limits. The data were presented in this manner despite the limits because in the absence of other information the Gaussian distribution is the first natural approximation.

(2) A second problem of significance is the determination of the values of the diffusion parameters. A Fick type process was assumed in the diffusion model for the fast fluctuations, and the error ranges are large. As has already been discussed by Gottfried and Haas (1992), the resolution of the diffusion parameter by global analysis of measurements, obtained with the present experimental system (pair of probes), was very limited. The error intervals were large, and in most experiments the conclusions of the present discussion are not based on the calculated diffusion parameters. There are probably large differences in the magnitude of the diffusion coefficients of the two subpopulations. The values of the diffusion parameters are presented in Table 2 for qualitative discussion only.

Structural Interpretation of the Results. With the limitations of the resolution of the determinations in mind, the main observations and conclusions found in the present experiments are summarized below:

Subpopulations. Most of the experiments reported here could not be fitted using a model consisting of a distribution of a single component, as has already been reported for measurements carried out under unfolding conditions (Amir et al., 1992; Gottfried & Haas, 1992). This is not a result of an error in the method. When the same derivatives were measured and analyzed by the same procedures in the native state, the time resolved experiments could easily be fitted by a narrow distribution of a single component. The existence of at least two subpopulations in the unfolded and partially folded states of BPTI means that the folding transition is not a continuum of partially folded states, but rather a set of specific structures stabilized by specific interactions with a range of equilibrated local substructures. Subpopulations were also found in the partially unfolded states of ribonuclease A and other examples (Sosnik & Trewhella, 1992; Shortle, 1993; Neri et al., 1992; Flanagan et al., 1993; Kataoka et al., 1993).

In the R state (at low GuHCl concentration, at pH 3.6) reduced BPTI has a major fraction of compact conformers and is not unfolded. An equilibrium between at least two subpopulations was found: a subpopulation of compact native-like conformers and a second subpopulation of conformers with expanded EED distribution, probably unfolded.

The main parameter that was affected by changes of either the solvent composition or the temperature was the probability ratio between the two subpopulations.

In the U state at 2 °C, the average transfer efficiency within the 46 residue segment was similar to that of the 26 residue segment. The dilution of the denaturant (transition to the R state) resulted in reduction of the size of the unfolded subpopulation. This change was much more pronounced for the longer (46 residues) segment. This means that, even under very destabilizing conditions, the longest possible loop in BPTI, between the two chain termini, is populated more than expected by unordered hydrophobic collapse. The order found in the R state is contributed by local interactions and also by NLIs between ends of long segments which thus form collapsed loops. The loop in the 46 residue segment was even more stable than the shorter 26 residue loop, under the influence of low pH (the A1 and A2 states) or increased temperature.

The temperature and pH dependence experiments may indicate some characteristics of the NLIs which stabilize the loops, but these should be considered only as clues to be used for design of specific tests and not as solid evidence. The cold unfolding which was found in the U state (Gottfried & Haas, 1992) was not observed in the R state.

Latman and co-workers report simulations of compact denatured states of proteins which also show bimodal distance distributions (Latman et al., 1994). Their interpretation is based on the assumption that two hydrophobic clusters are formed. This does not seem to be the case here, and we interpret the results in terms of the contribution of specific NLIs. This specificity of the interactions is in agreement with the arguments of Latman and Rose, who suggested that a specific stereochemical code directs the folding (Latman & Rose, 1993).

Loop Closure by Specific NLIs in the Partially Folded States. In the R state the main subpopulations of 26, 41, and 46 residue segments were centered around 20 Å, very close to the native distances. This is clearly not a case of a simple condensation by hydrophobic collapse but rather has features of native topology. The 1−15 segmental EED was different; its major subpopulation had a non-native EED. The average of this EED distribution was shorter than the native length. The largest change of conformation associated with the transition from the U to the R state was found in long segments, the 41 and 46 residues in which the unfolded subpopulation decreased to ca. 10% by the transition to the partially folding conditions (R state). Examination of these two segments in Figure 1 shows that they can be viewed as comprising long range loops whose ends are in contact. The same is true for the 26 residue segment, while the 15 residue segment is relaxed into an unordered structure. The first three longer segments can be viewed as forming, in the R state, long loops. The loops are defined by the interactions which hold the ends of the segments in close contact, by very effective nonlocal interactions (NLIs). The middle of the segments between the interacting ends are either folded by LIs or other NLIs or randomly condensed into the compact structures by the hydrophobic collapse, as can be the case of the 15 residue segment (N loop). A similar contribution can be involved in the stabilization of the short 1−41 EED (collapse of the C loop). Figure 1 shows that in BPTI two stable NLIs, one between the terminal segments (γ and α, represented by the proximity of residues 1 and 46) and one between the same termini and the central part of the chain (β) (including residue 26), can force the molecule into native-like topology of two major loops (residues 1−26 and 26 to the N terminus). The combination of the two loops forms an overall loop of the whole chain, which is stabilized even under partially folding conditions.

This observation may be relevant to the question of the pathway of folding. It is possible that the design of the protein molecule includes the strongly interacting ends of segments, in order to form closed loops at high efficiencies in the early folding intermediates. Such loops can be very effective means for major reduction of the chain entropy, at the expense of a single NLI each. This structure is describes as a "loop" since the flexibility of the 1−15 EED distance shows that, at least in this case, the chain segment between the two interacting ends has a distribution which can be that of a statistical coil. Therefore, the definition of the loop here is a chain segment whose ends are held in the close proximity by an NLI, and the rest of the chain between the interacting ends can be in any conformation. There are probably few LIs that are effective in directing the topology of the chain in the folding intermediates as well as in the R state. The most obvious candidates are the LIs that stabilize secondary structures. Yet, even in the absence of additional LIs, the closure of the long loops can force the chain into a native-like overall topology.

This view is supported by the results of the search for secondary structures in the R state. Gussakovasky and Haas (1991) used ORD measurements in searching for secondary structures in reduced BPTI in the U and R states. No signal for such structures was found. More recently, Lumb and Kim (1994) used 2-D NMR in the search for secondary structures in an all-Ala-BPTI, a model of reduced BPTI similar to the R state, and also did not find any signal of such structures. That means that the structures detected in the present experiment are not dependent on secondary structures. In the partially folded state, these structures are stabilized by the NLIs between the three segments which form the main structural elements of the native conformation.

What are the NLIs which lock the loops in the partially folded states? Woodward and her collaborators (Kim et al., 1993) studied the mechanism of hydrogen exchange in BPTI and proposed that the protein segments in the slow exchange core determine the basic fold of the protein and that, in compact non-native states, the collapsed region corresponds to the slow exchange core. The slow exchange core revealed by the NMR experiments is located at the ends of the loops observed here and involves residues 21−24, 30−33 (part of β, close to 26), 43−45, and 51 (part of α and the N-terminal segment, near 46) (Kim et al., 1993). The loops between the segments locked in the slow exchange core (9−17 and 36−43) showed fast exchange. According to Kim et al. the slow exchange core in BPTI is the folding core, and they propose that it is packed by hydrophobic side chains of residues involved in secondary structures. The loops and the folding core proposed by Kim et al. are very close to the loops and their interacting ends found in the U and the R states by the ET experiments. This supports the proposed interpretation that the NLIs which close the loops in the R state include strong contribution of hydrophobic interactions. Yet, in the partially folded states investigated here this core does not include stable secondary structures; these probably form under less denaturing conditions, and the role of the NLIs is further emphasized.

Folding Units. Kim et al. (1993) proposed that folding proceeds in stages: collapse of the slow exchange core, followed by packing of secondary structure elements not in the core and packing of the flexible loops. The present experiments are in line with this proposal. Based on the current ET experiments, it is proposed that *the collapse of the core is directed by the closure of the loops by specific NLIs, prior to formation of secondary structures of the core*, and then the pathway proceeds as proposed by Kim et al. Moreover, since the NLIs direct the formation of the core by the closure of the loops, a possible definition for a basic folding unit of globular proteins is proposed here: *The basic folding unit of a globular protein can be defined by the longest loop whose ends are held by specific NLIs which are strong enough to be effective under conditions of overall unfolding*, partially folding conditions, or the initial intermediates of the folding pathway. In the case of BPTI, these NLIs are involved in formation of the core. The longest loop includes the whole chain, since the segment from 1 to 46 forms the longest loop in the R state. In other proteins the longest segment which makes loops with interacting ends can be less than the full length of the chain, and in such a case the protein may have more than one folding unit.

The probability for loop closure by random encounter of the ends of an oligomer within the time scale of the initial folding transitions (submillisconds) is high (Winnik, 1981). The rate of cyclization is estimated to be faster than microseconds. Thus, the rate of encounters of the ends of chain segments for loop closure is not the limiting factor in loop formation. This is the case if the interacting groups at the segments' ends interact in an attractive mode, even under nonfolding conditions (no disulfides, low pH, and low GuHCl concentration). Pairs of groups of side chains which interact via hydrophobic or polar interactions can stabilize loops formed randomly in the collapsed state. It is further proposed that loop formation is a very effective means of reducing chain entropy at the expense of a minimal number of very stable interactions.

In a similar study (Buckler, unpublished results) it was found that the two terminal chain segments of reduced RNase A, under partially folding conditions, do not have a strong NLI which brings them to a native-like distance. RNase A probably contains more than one initial loop and therefore consists of more than one folding unit.

The importance of early formation of long range loops in the folding pathway of model protein chains was also demonstrated in simulation studies (Dagget & Levitt, 1992; Sali et al., 1994). Shakhnovich has observed that formation of one long loop can initiate a rapid collapse into a compact conformation which is then followed by a slow search for the detailed exact folding (E. Shakhnovich, personal communication). Levitt has reported a simulation of the folding of a simplified BPTI model in which he observed early compaction of the chain with stable interactions between the α and the β segments (M. Levitt, personal communication).

The obvious next question is whether the topology of the intermediates is native-like. This question is equivalent to the question whether subdomain folding occurs by stabilization of native conformation of structural elements early in the folding pathway. The present method gives partial answers to these questions in some cases. Note, for example, the native-like EED distributions of the first subpopulations in the 26, 41, and 46 residue segments. Figure 1 shows that the native topology of BPTI is characterized by the proximity of the three segments, α, β, and γ, thus forming two loops (N and C) between them. In BPTI two *NLIs which connect the ends of the loops sufficiently restrict the conformational space and force the protein into an ensemble of conformations very close to the native one.* In the absence of an interaction between the two "turns" in the loops (residues 12−17 and 37−42, respectively) the chain is relaxed into a spherical globule rather than the oblate native structure seen in Figure 1.

CONCLUSIONS

The present set of experiments shows that major features of the topology of the backbone of BPTI are native-like even under unfolding and partially folding conditions. It is conceivable that these features are also essential elements of the folding pathway of the protein. The long range nonradiative ET measurements were effective in revealing the loops formed in the unfolded and partially folded states even in the absence of disulfide cross links. One of the goals of the present experiments was to search for a molten globule (MG) state of BPTI and the topology of the chain in that state. It is not clear whether the MG state is properly defined under the present conditions (Gussakovsky & Haas, 1992), but the topology is native-like even in the partially folding conditions investigated here.

The main conclusion from the present study is that *loop formation by specific NLIs can be a key factor in the solution of the so-called Levinthal paradox* and in determining the steps which direct the folding pathway. The loops are generated by loose cross links between pairs of specific sites (pairs of single residues or short stretches of the chain). This brings about a major reduction in chain entropy and reduction in the size of the searched conformational space. The next obvious step is to search for the specific residues that contribute the NLIs between the ends of each loop and in particular those which define the folding units in each protein. The combination of site directed mutagenesis and a long

range ET detection method seems to be a promising approach to this question.

ACKNOWLEDGMENT

We wish to thank Drs. G. L. Haberland and E. Wischofer of A. G. Bayer for the generous gift of Trasylol®. We thank D. S. Gottfried, D. Amir, G. Haran, and R. Horwitz for continuous interest and helpful discussions. The technical assistance of Mr. D. Freedman, E. Zimmerman, and L. Varshavasky is gratefully acknowledged.

REFERENCES

Alonso, D. D., Dill, K. A. & Stiger, D. (1991) *Biopolymers 31*, 1631−1649.
Amir, D., & Haas, E. (1987) *Biochemistry 26*, 2162−2175.
Amir, D., & Haas, E. (1988) *Biochemistry 27*, 8889−8893.
Amir, D., Krausz, S., & Haas, E. (1992) *Proteins 13*, 162−173.
Beals, J. M., Haas, E., Krausz, S., & Scheraga, H. A. (1991) *Biochemistry 30*, 7680−7692.
Beechem, J. M., & Haas, E. (1989) *Biophys. J. 55*, 1225−1236.
Berndt, K. D., Güntert, P., Orbons, P. M., & Wüthrich, K. (1992) *J. Mol. Biol. 227*, 757−775.
Chaffotte, A. F., Cadieux, C., Gullou, Y., & Goldberg, M. E. (1992) *Biochemistry 31*, 4303−4308.
Chen, S. U., Cheng, K. H., & Van Der Meer, B. (1992) *Biochemistry 31*, 3759−3768.
Creighton, T. E. (1978) *Prog. Biophys. Mol. Biol. 33*, 231−297.
Creighton, T. E. (1980) *J. Mol. Biol. 144*, 521−550.
Creighton, T. E. (1984) *Proteins*, Freeman, San Francisco.
Creighton, T. E. (1986) Disulphide Bonds as Probes of Protein Folding Pathway. In *Methods in Enzymology* (Hirs, C. H. W., & Timashef, S. N., Eds.) Vol. 131, pp 83−106, Academic.
Dagget, V., & Levitt, M. (1992) *Proc. Natl. Acad. Sci. U.S.A. 89*, 5142−5146.
Dale, R. E., Eisinger, J., & Blumberg, W. E. (1979) *Biophys. J. 26*, 161−194.
Danishefsky, A. T., Hausset, D., Kim, K. S., Tao, F., Fuchs, J., Woodward, C., & Wlodawer, A. (1993) *Protein Sci. 2*, 577−587.
Darby, N. J., van-Mierlo, C. P. M., & Creighton, T. E. (1991) *FEBS Lett. 279*, 61−64.
Darby, N. J., van-Mierlo, C. P., Scott, G. H., Neuhaus, D., & Creighton, T. E. (1992) *J. Mol. Biol. 224*, 905−911.
Deisenhofer, J., & Steigemann, W. (1975) *Acta Crystallogr. B 31*, 238−250.
Dill, K. A., & Shortle, D. (1991) *Annu. Rev. Biochem. 6*, 795−825.
Dobson, C. M. (1991) *Curr. Opin. Struct. Biol. 1*, 22−27.
Flanagan, J. M., Kataoka, M., Fujisawa, T., & Engleman, D. M. (1992) *Proc. Natl. Acad. Sci. U.S.A. 32*, 10359−10370.
Forster, Th. (1948) *Ann. Phys. (Leipzig) 2*, 55−75.
Goldenberg, D. P., & Zhang, J. X. (1993) *Proteins 15*, 322−329.
Goldenberg, D. P., Berger, J. M., Laheru, D. A., Wooden, S., & Zhang, J. X. (1992) *Proc. Natl. Acad. Sci. U.S.A. 89*, 5083−5087.
Goto, Y., & Fink, A. L. (1989) *Biochemistry 28*, 945−952.
Goto, Y., & Fink, A. L. (1990) *J. Mol. Biol. 214*, 803−805.
Gottfried, D. S., & Haas, E. (1992) *Biochemistry 31*, 12353−12362.
Grinvald, A., & Steinberg, I. Z. (1974) *Anal. Biochem. 59*, 583−598.
Gussakovsky, E. E., & Haas, E. (1992) *FEBS Lett. 2*, 146−148.
Haas, E. (1986) in *Photophysical and Photochemical Tools in Polymer Science* (Winnik, M. A., Ed.) pp 310−341, D. Reidel, Dordrecht.
Haas, E., Wilchek, M., Katchalski-Katzir, E., & Steinberg, I. Z. (1975) *Proc. Natl. Acad. Sci. U.S.A. 72*, 1807.
Haas, E., Katchalski-Katzir, E., & Steinberg, I. Z. (1978a) *Biopolymers 17*, 11−31.
Haas, E., Katchalski-Katzir, E., & Steinberg, I. Z. (1978a) *Biochemistry 17*, 5064.
Harrison, S. C., & Durbin, R. (1985) *Proc. Natl. Acad. Sci. U.S.A. 82*, 4028−4030.
Hillel, Z., & Wu, C. W. (1976) *Biochemistry 15*, 2105−2112.
Housset, D., Kim, K. S., Fuchs, J., Woodward, C., & Wlodawer, A. (1991) *J. Mol. Biol. 220*, 757−770.
Hurle, M. R., Marks, C. B., Kosen, P. A., Anderrson., S., & Kunts, I. D. (1990) *Biochemistry 29*, 4410−4419.
James, D. R., Demmer, D. R. M., Verrall, R. E., & Steer, R. P. (1983) *Rev. Sci. Instrum. 54*, 1121−1130.
James, E., Wu, P. G., Stites, W., & Brand, L. (1992) *Biochemistry 31*, 10217−10225.
Jones, R. E. (1970) Nanoseconds Fluorimetry, Ph.D. Thesis, Stanford University.
Karplus, M., & Weaver, D. L. (1976) *Nature 260*, 404−406.
Karplus, S., Snyder, G. H., & Sykes, B. D. (1973) *Biochemistry 12*, 1323−1329.
Kataoka, M., Hagihara, Y., Mihara, K., & Goto, Y. (1993) *J. Mol. Biol. 229*, 591−596.
Kim, K. S., Fuchs, J. A., & Woodward, C. K. (1993) *Biochemistry 32*, 9600−9608.
Kim, P. S., & Baldwin, R. L. (1990) *Annu. Rev. Biochem. 59*, 631−660.
Kobayashi, Y., Sasabe, H., Akutsu, T., & Saito, N. (1992) *Biophys. Chem. 44*, 113−127.
Kuwajima, K. (1989) *Proteins: Struct., Funct., Genet. 6*, 87−103.
Latman, E. E., & Rose, D. G. (1993) *Proc. Natl. Acad. Sci. U.S.A. 90*, 439−441.
Latman, E. E., Fiebig, K. M., & Dill, K. (1994) *Biochemistry 33*, 6158−6166.
Levinthal, C. (1968) *J. Chim. Phys. 85*, 44−45.
Levitt, M. (1983) *J. Mol. Biol. 170*, 723−764.
Lumb, K. J., & Kim, P. S. (1994) *J. Mol. Biol. 236*, 412−420.
Manning, M. C., & Woody, R. W. (1989) *Biochemistry 28*, 8609−8613.
Masson, A., & Wüthrich, K. (1973) *FEBS Lett. 31*, 114−118.
Matthews, C. R. (1991) *Curr. Opin. Struct. Biol. 1*, 28−35.
Montelione, G. T., & Scheraga, H. A. (1989) *Acc. Chem. Res. 22*, 70−76.
Neri, D., Billeter, M., Wider, G., & Wüthrich, K. (1992) *Science 257*, 1559−1563.
Ptitsyn, O. B. (1987) *J. Protein Chem. 6*, 273−293.
Roeder, H., Elove, G. A., & Englander, S. W. (1988) *Nature 335*, 694−699.
Sali, A., Shakhnovich, E., & Karplus, M. (1994) *J. Mol. Biol. 235*, 1614−1636.
Sancho, J., Neira, J. L., & Fersht, A. R. (1992) *J. Mol. Biol. 224*, 749−758.
Schmid, F. X. (1992) *Curr. Opin. Struct. Biol. 2*, 21−25.
Shortle, D. (1993) *Curr. Opin. Struct. Biol. 3*, 66−74.
Shortle, D., & Meeker, A. K. (1989) *Biochemistry 28*, 936−944.
Sosnik, T. R., & Trewhella, J. (1992) *Biochemistry 31*, 8329−8335.
Stiger, D., Alonso, D. O. V., & Dill, K. A. (1991) *Proc. Natl. Acad. Sci. U.S.A. 88*, 4176−4180.
Stryer, L. (1978) *Annu. Rev. Biochem. 47*, 819−846.
Stryer, L., & Haugland, R. P. (1967) *Proc. Natl. Acad. Sci. U.S.A. 58*, 719−726.
Tanford, C. (1968) *Adv. Protein Chem. 23*, 121−282.
Tüchsen, E., & Woodward, C. (1987) *J. Mol. Biol. 193*, 793−802.
Uversky, V. N., Semistonov, G. V., Pain, R. H. & Ptitsyn O. B. (1992) *FEBS 1*, 89−92.
Van Mierlo, C. P. M., Darby, N. J., Neuhaus, D., & Creighton, T. E. (1991) *J. Mol. Biol. 222*, 373−390.
Van Mierlo, C. P. M., Darby, N. J., Keeler, J., Neuhaus, D., & Creighton T. E. (1993) *J. Mol. Biol. 229*, 1125−1146.
Wagner, G., Brühwiler, D., & Wüthrich, K. (1987) *J. Mol. Biol. 196*, 227−231.
Weissman, J. S., & Kim, P. S. (1991) *Science 253*, 1386−1393.
Weissman, J. S., & Kim, P. S. (1992) *Science 256*, 112−114.
Winnik, M. A. (1981) *Chem. Rev. 81*, 491−524.
Wlodawer, A., Walter, J., Huber, R., & Sjolin, L. (1984) *J. Mol. Biol. 180*, 301−329.
Wlodawer, A., Nachman, J., Gilliland, G. L., Gallagher, W., & Woodward C. (1987) *J. Mol. Biol. 198*, 469−480.
Yang, A. S., & Honig, B. (1992) *Curr. Opin. Struct. Biol. 2*, 40−45.
Zuker, M., Szabo, A. G., Bramall, L., & Krajcarski, D. T. (1985) *Rev. Sci. Instrum. 56*, 14−22.

BI941907A